Design of a Quadratic, Antagonistic, Cable-Driven, Variable Stiffness Actuator

Ryan Moore
Department of Mechanical Engineering,
Marquette University,
Milwaukee, WI 53233
e-mail: ryan.moore@marquette.edu

Joseph M. Schimmels
Department of Mechanical Engineering,
Marquette University,
Milwaukee, WI 53233
e-mail: j.schimmels@marquette.edu

Antagonistically actuated variable stiffness actuators (VSAs) take inspiration from biological muscle structures to control both the stiffness and positioning of a joint. This paper presents the design of an elastic mechanism that utilizes a cable running through a set of three pulleys to displace a linear spring, yielding quadratic spring behavior in each actuator. A joint antagonistically actuated by two such mechanisms yields a linear relationship between force and deflection from a selectable equilibrium position. A quasi-static model is used to optimize the mechanism. Testing of the fabricated prototype yielded a good match to the desired elastic behavior. [DOI: 10.1115/1.4050104]

Keywords: robotics, compliance, antagonistic, variable stiffness actuators, actuators and transmissions, bio-inspired design, cable-driven mechanisms, compliant mechanisms, mechanism design

1 Introduction

Robotic compliance is a key area of research due to its importance in both (1) improving the performance of robotic manipulators in a range of manipulation tasks, especially those with changing or uncertain constraint conditions and (2) improving the safety of manipulators during interactions with other parts, other robots, or human collaborators [1].

The two options for realizing compliant behavior in a robotic mechanism are active compliance control and intrinsic (passive) compliance. Active control involves the use of sensors to monitor forces acting on the manipulator and controlling the actuators to compensate for these contact forces by moving the manipulator in order to simulate physical springs built into the system. This strategy is commonly used by collaborative robots on the market today.[1]

Intrinsic compliance can be incorporated using springs or other elastic components built into the actuator (series elastic actuators) or, more commonly, built into the end effector. The "Remote Center Compliance System" [2] was one of the first frameworks for such a system in which task-specific end effector compliant tooling was created. Variable stiffness actuators (VSAs) are a form of series elastic actuators in which both the position and the stiffness of the joints are controlled [3]. VSAs can change the compliance in real-time to safely perform a variety of tasks without the downtime required when changing the passive end of arm tooling or with the lag and dynamic instability inherent in active compliance control.

The Flexible Antagonistic Spring Element (FAS) designed by the German Aerospace Center (DLR) [4–6], depicted in Fig. 1, provides a large range of stiffness and large allowable compliant deflection from equilibrium. This mechanism design, used in each joint of the DLR Hand Arm System, incorporates two antagonistic lever and pulley-cable systems to obtain a range of stiffness behavior from the extension of a linear extension spring.

In each of the two (upper and lower) drive components illustrated in Fig. 1, a cable is connected on one end to a motorized pulley, wrapped around a compliantly constrained spring pulley, then wrapped around a constrained guide pulley, and connected on the other end to a link (link i) around a rotational joint. As the cable length between the motor pulley and the fixed pulley is shortened or extended (either through the movement of the motor pulley or rotation of link i), the lever connecting the spring pulley and fixed pulley rotates and produces a force in the attached linear spring. The two drive components together constitute a VSA capable of both passive stiffness modulation and position control of the joint.

The DLR actuation strategy minimizes the inertia of the joint while achieving a large range of stiffness in a compact mechanism. Low inertia at the joint of the mechanism is useful in improving the safety of the mechanism. Additionally, the lower inertia at the joint of the mechanism reduces the torque requirements of the motors

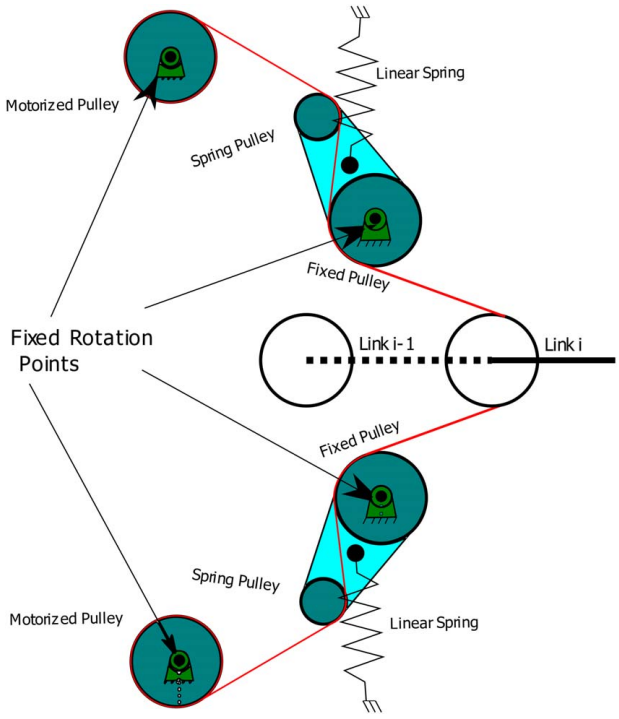

Fig. 1 DLR's flexible antagonistic spring element design

[1] https://www.franka.de/technology, https://www.universal-robots.com/products/ur10-robot/, https://www.kuka.com/en-us/products/robotics-systems/industrial-robots/lbr-iiwa

Contributed by the Mechanisms and Robotics Committee of ASME for publication in the Journal of Mechanisms and Robotics. Manuscript received September 25, 2020; final manuscript received January 25, 2021; published online March 12, 2021. Assoc. Editor: Philip A. Voglewede.

used in the design, reducing the overall cost of the design. By relocating the motors and stiffness controlling mechanisms away from the controlled joint, the mass and mass moment of inertia of the controlled joint will be reduced. Improving the compactness of the VSA design is an important design objective as it improves the feasibility of implementing the design into real-world systems.

Each of the two lever and pulley systems achieves nonlinear stiffness behavior that increases stiffness by increasing the tension in each of the two cables attached to the link. The nature of the DLR stiffness nonlinearity, however, was not specified.

An important criterion in the design of *elastic* mechanisms is the relationship between torque and angular deflection given a controlled equilibrium position. A linear joint stiffness is desirable because it results in a constant value when the joint is deflected and can simplify the complexity and cost of the control system used to control the mechanism.

The main objectives of this work are to (1) refine the DLR actuator strategy to achieve elastic performance that is easier to specify and control and (2) validate theoretical results experimentally. The refined design achieves both (1) a large range in stiffness through coactivation and (2) a large range of linear elastic behavior when the joint is deflected from equilibrium.

Figure 2 shows the layout of the nonlinear elastic mechanism for which the mechanism's geometric parameters (e.g., pulley locations and sizes) were optimized so that when paired with an opposing mechanism a linear stiffness at the robotic joint is obtained. Similar to the DLR's FAS design, the developed mechanism utilizes a cable (solid lines) routed through a set of three pulleys. Tension on the cable imposed at the cable-free end displaces a linear extension spring, causing the spring pulley to move along the arc (dashed line) to produce a nonlinear tension-deflection at the cable end. The stiffness of the mechanism is characterized by this force-deflection relationship as seen at the free end of the cable, where the external force is applied.

The design differences between the DLR system and the new VSA design (shown in Fig. 2) were made primarily for consistency in comparing results with a competing mechanism design (not presented here). The point where the linear spring attaches to the lever was moved to the center of the spring pulley in order to ensure no interference between the spring subsystem and the lever-pulley subsystem as the lever moves. The lever base was moved to provide rotation about the motor pulley rather than the guide pulley. This relocation of the lever plays no role in the mechanism analysis (and subsequent optimization) since the geometry of the lever-pulley subsystem is effectively just the mirror image of the existing FAS design.

This investigation into the feasibility, effectiveness, and optimization of an antagonistic quadratic spring system to achieve an effective linear stiffness at the robotic joint is the main goal of this paper.

This paper is structured as follows: Sec. 2 introduces the mathematics of the quasi-static model of the mechanism as well as the optimization methodology used to achieve the desired elastic behavior of the system. Section 3 provides an overview of the prototype testing system and the key design decisions for the prototype implementation. Section 4 discusses the prototype testing methodologies and results, and Sec. 5 concludes the paper with a summary.

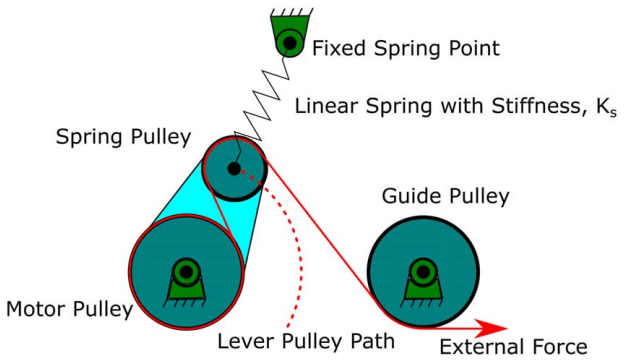

Fig. 2 One side of the antagonistic, quadratic stiffness cable-driven VSA design

2 Antagonistic Quadratic Elastic Behavior

The objective of this VSA mechanism is to produce a desired nonlinear force-deflection behavior with a single lever and pulley system. The desired nonlinear stiffness in translation is given by

$$F = K\ sgn(x - x_C)(x - x_C)^2 \tag{1}$$

where $(x - x_C)$ is the deflection from the commanded position.

When two of these VSA mechanisms with signed quadratic force-deflection relationships are attached antagonistically to a joint, the resulting stiffness of the joint is linear [7]. This relationship is shown in Fig. 3 and Eqs. (2)–(5):

The constitutive equations for the two springs when $x > x_L$ and $x < x_R$ are

$$F_1 = K(x - x_L)^2 \tag{2}$$

$$F_2 = -K(x - x_R)^2 \tag{3}$$

The combination of forces acting on the link yields

$$F_1 + F_2 = K(x^2 - 2xx_L + x_L^2 - x^2 + 2xx_R - x_R^2) \tag{4}$$

$$F_1 + F_2 = 2K(x_R - x_L)\left[x - \frac{1}{2}(x_L + x_R)\right] \tag{5}$$

Note that the effective stiffness of the two quadratic springs working antagonistically is linear. The effective stiffness of the joint is $K_j = 2K(x_R - x_L)$ and the controlled equilibrium position is $x_c = 1/2(x_L + x_R)$.

The two motors in Fig. 1 are the equivalent of the two actuators of Fig. 3. When the two motors both pull the cable causing the cable to spool on the motor pulley an equal amount, the effective stiffness of the system at the cable end is increased. If the motors cause one cable to spool and the other to unspool the same amount, the link position is changed but the stiffness is unchanged.

A quasi-static model of the elastic lever/pulley system was developed to evaluate the tension on the cable at any given motor position combination (x_R, x_L), as well as, the deflection of the cable from its original neutral position. This position is obtained when there is no tension (or equal tension) on the mechanism cables. The neutral position (zero stiffness) of the mechanism is obtained when the center of the motor pulley, center of the spring pulley, and fixed end of the linear spring are collinear, for which case, the spring force and spring pulley path are orthogonal.

In Fig. 4, the forces acting on the spring pulley center are displayed along with the available direction of motion at the neutral mechanism position. F_S is the force acting on the pulley due to the extension of the spring, F_N is the force acting on the pulley due to the interactions between the pulley and the lever preventing it from moving off the arc path of the lever, and T_1 and T_2 are the forces acting on the pulley due to the cables wrapping over the pulley and extending toward the motor pulley and guide pulley, respectively. The direction of motion is always perpendicular to

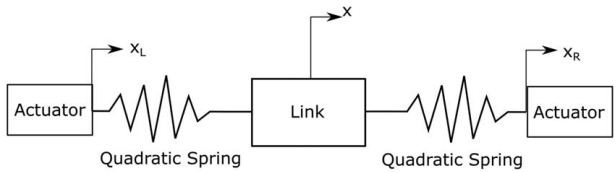

Fig. 3 Translational opposing quadratic spring configuration

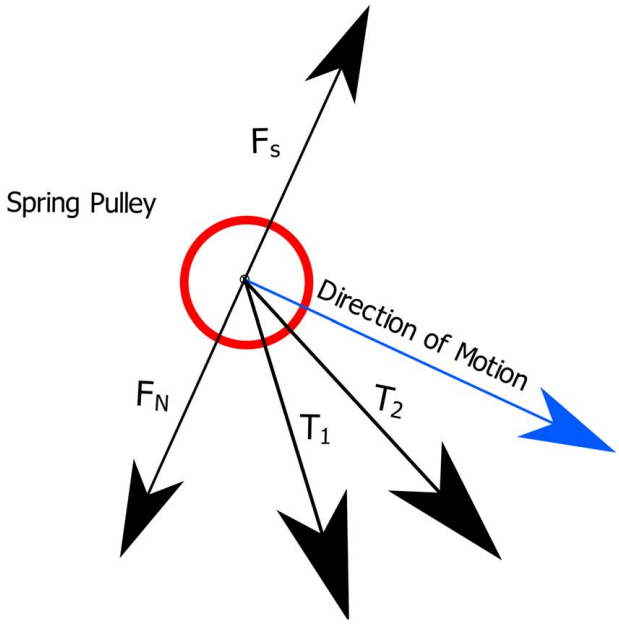

Fig. 4 Free body diagram of the pin joint on the spring pulley

F_N, the normal force provided by the mechanism lever. When there is tension in the cables, F_S and F_N are no longer collinear.

If the locations of the pulleys, the fixed point of the linear spring, and the stiffness of the linear spring (as indicated in Fig. 2) are known, then, the two unknown values in the system, the magnitudes of the normal and cable tension forces, can be resolved using the following equations.

$$\boldsymbol{T}_1 + \boldsymbol{T}_2 + \boldsymbol{F}_N + \boldsymbol{F}_s = 0 \tag{6}$$

$$T = T_1 = T_2 \tag{7}$$

$$\begin{bmatrix} (T_{1x} + T_{2x}) & F_{Nx} \\ (T_{1y} + T_{2y}) & F_{Ny} \end{bmatrix} \begin{bmatrix} T \\ F_N \end{bmatrix} = \begin{bmatrix} -F_s F_{sx} \\ -F_s F_{sy} \end{bmatrix} \tag{8}$$

where, for example, the force vector $\boldsymbol{T}_1$ has magnitude T_1 and direction $[T_{1x}, T_{1y}]$.

The other value required to determine the force-deflection behavior of the mechanism is the deflection of the mechanism at any given configuration. This is done by comparing the length of the cable in the mechanism to the length of the cable in the mechanism in its no-load position. Segments AB, CD, and EF, in Fig. 5, are calculated as arc lengths given the radii of the respective pulleys and the tangent points of the cable lines between the pulleys. Segments BC and DE are calculated as the distance between the two tangent point locations.

Eight parameters are used to model the force-deflection relationship of the mechanism. This model is foundational in the optimization of the mechanism geometry to produce the desired quadratic force-deflection behavior necessary for linear joint elastic behavior. Figure 6 illustrates the seven geometric parameters used in the mechanism elastic model.

The eight model parameters are:

- R_M: normalized radius of the motor pulley attached to the motor and one end of the cable
- R_S: normalized radius of spring pulley that follows the lever path
- R_G: normalized radius of the guide pulley directing the cable towards the link at which the other end of the cable is attached
- R_I: normalized lever length: the distance between the center of the motor pulley and spring pulley
- L_0: normalized free length of the spring

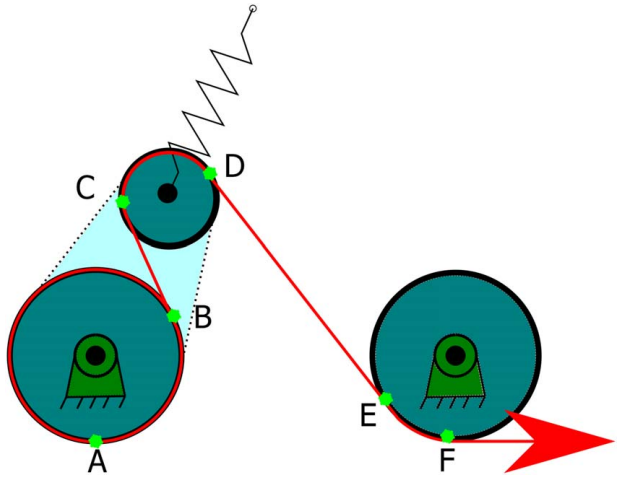

Fig. 5 Cable length segments

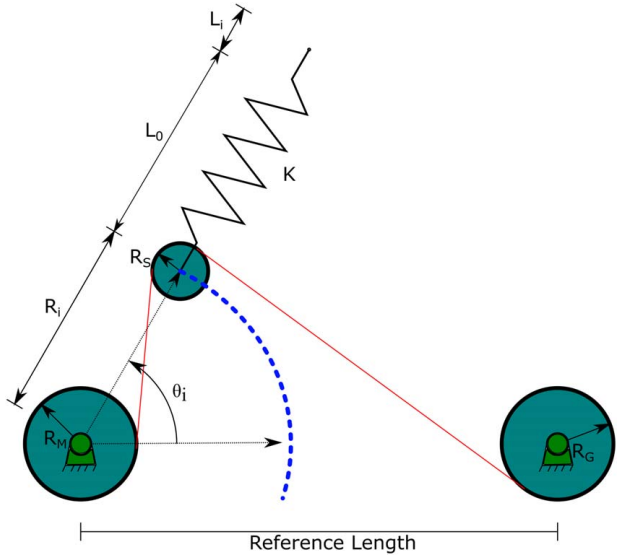

Fig. 6 Mechanism design parameters

- θ_i: the initial angle between the x-axis and the line connecting the centers of the motor and spring pulleys
- L_i: normalized initial extension of the spring from its free length
- K: linear spring stiffness

Note that all model distance parameters are normalized relative to the horizontal distance between the center of the motor pulley and guide pulley.

The elastic model of the VSA mechanism was then optimized to find the parameters that yield the force-deflection behavior that best matches the desired quadratic force-deflection behavior. For each design evaluation, the path of the spring pulley, from the zero-stiffness position to the fully taut position, was divided into 1000 points, and the change in cable length within the mechanism and the cable tension was calculated for each position.

The optimization algorithm evaluated the 1000 points along the deflection path and determined the longest consecutive range of cable deflection values (i.e., the largest number of sequential points) that fell within the selected error band of the linear stiffness-deflection line. This number was used as the optimization's objective function value.

Two constraints were placed on the mechanism geometry to ensure the mechanism does not collide with itself as the cable is

Table 1 Optimal geometric parameters

Design parameter	Optimized value
R_M	0.2394
R_S	0.1498
R_G	0.2320
R_I	0.4958
L_o	0.5798
θ_i	64.663
L_i	0.0

pulled. Equations (9) and (10) constrain the lever length and the radii of the spring pulley, motor pulley, and guide pulley to ensure they do not collide.

$$R_M + R_S - R_I < -0.1 \tag{9}$$

$$R_S + R_G + R_I \cos(\theta_i) < 0.95 \tag{10}$$

The design space proved to be highly nonlinear and multiple different strategies were used to find an optimal value (e.g., genetic algorithms, multi-start and global search sequential quadratic programming). Many spurious local minima were identified. The best result of the many optimization results is described below.

Table 1 shows the optimal geometric parameters normalized relative to the horizontal distance between the center of the motor pulley and guide pulley. Figure 7 shows the relative sizing of the optimized geometric parameters in the final design of the VSA mechanism.

Figure 8 shows the force-deflection curve of the optimized design along with the target quadratic elastic behavior. The dimensionless deflection values indicate the deflection of the cable end from its no-load state. This parameter is dimensionless because it is scaled by the size of the mechanism. Here, size is characterized by the distance between the motor pulley and the guide pulley. Force is normalized by the spring constant K and normalized deflection.

The range of acceptable deflections in which the mechanism matched the desired stiffness was between a deflection of approximately 0.25 and a deflection of 0.75. Figure 9 shows the optimized mechanism's deflection versus stiffness curve. It also shows the desired deflection versus stiffness line and an error bound of ± 0.05 from the acceptable value. This error bound was selected as it was the tightest bound that still produced an acceptable region of significant length and broader error bounds produced deflection versus stiffness lines with worse linearity.

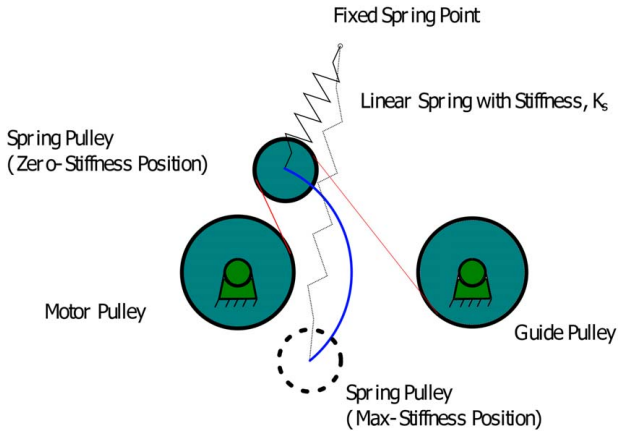

Fig. 7 Final mechanism configuration

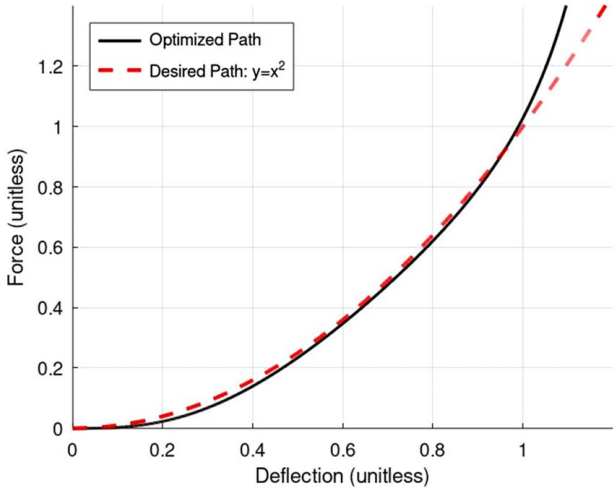

Fig. 8 Final mechanism force-deflection curve

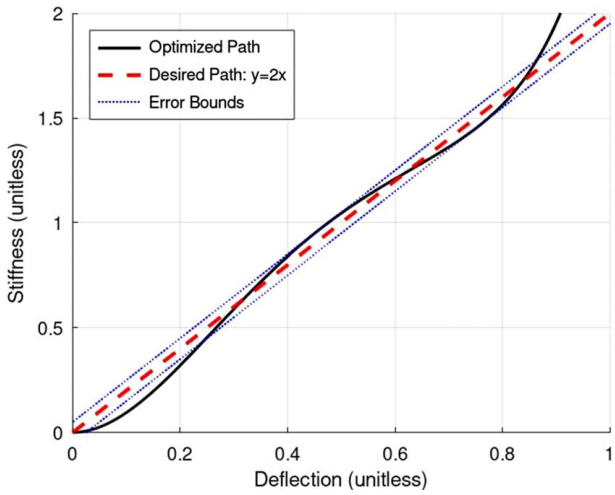

Fig. 9 Final mechanism stiffness-deflection curve

3 Physical Design and Implementation

The physical implementation of this VSA design consisted of the two VSA motors connected to cables, routed through the pulley-spring mechanism, and attached antagonistically to a single-joint robot finger. The test apparatus was scaled using a 50 mm length to substitute for the 1-unit reference length between the motor pulley center and guide pulley center. This sizing allowed for use of readily obtainable, off-the-shelf bearings and shafts to be used. This design can be scaled to other sizes depending on the application needs. Figure 10 shows the VSA connected to a link (1 DoF finger).

Functionally, this mechanism acts similarly to the agonist-antagonist principle that controls human muscle movement. A cable is attached to either side of the link across the joint and applied torque in opposing rotational directions. A motor controls the positioning of the ends of the cable on each (upper and lower) mechanism. As an example, when the cable on the bottom side of the mechanism is shortened, a torque is applied to the finger joint causing a downward rotation along with a stiffening of the mechanism.

Two DC motors with 150:1 ratio planetary gearheads and Maxon Motor's EPOS4 position control drives were selected to drive the VSAs. These motors were selected for their high torque to size ratio which allowed for enough torque to drive a robotic joint,

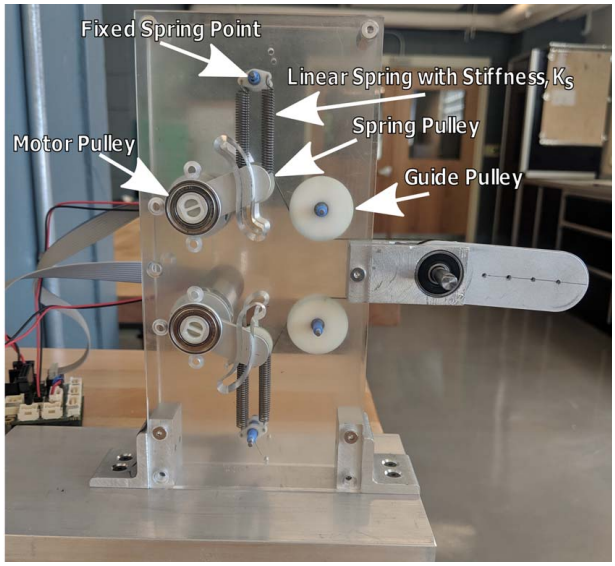

Fig. 10 Testing apparatus for VSA

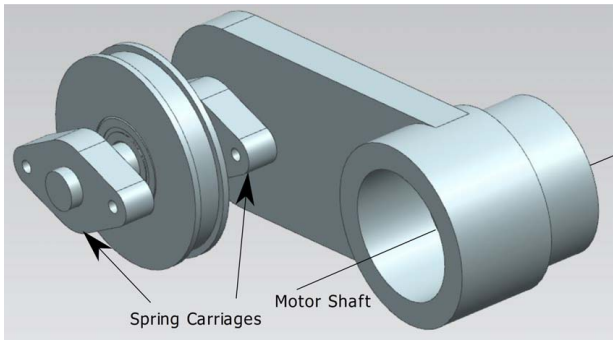

Fig. 11 Lever shaft assembly and spring carriage

approximately the length of an adult male's index finger, to lift at least 20 lbs.

In order to control the motion of the spring pulley, a lever was designed to rotate about the center of the motor pulley and move along the spring pulley's optimized arc. Figure 11 shows the lever design, along with the spring pulley mounted on the center of the shaft and two spring carriages used to affix the linear springs to the shaft.

Off-the-shelf linear extension springs were chosen for the mechanism. The available selection of spring stiffnesses and spring lengths was limited, and therefore, springs were chosen to match the requirements as closely as possible following these criteria.

- The allowable spring deflection must not exceed the manufacturer's specified maximum spring deflection in order to prevent plastic deformation.
- The spring should provide some preload to ensure spring tension throughout the range of motion.
- The stiffness of the spring should be as large as possible in order to achieve the largest range of linear stiffnesses.

Table 2 shows the desired characteristics of the linear spring versus the actual characteristics of the selected spring system. Because available spring values were limited, and no single spring satisfied both the acceptable maximum deformation and the spring rate, a system of four springs connected in parallel was used. Two springs were attached to each of the two spring carriages (one carriage on each side of the spring pulley as shown in Fig. 11) and the other end of the spring system was attached to the fixed spring point shown near the top of Fig. 10. The four-spring parallel

Table 2 Spring Characteristics

Spring characteristic	Desired	Actual
Spring length (mm)	28.83	25.40
Allowable deflection (mm)	27.84	27.94
Spring rate (N/mm)	3.74	0.473

system acts as a single spring with four times the spring constant. The overall spring rate of the system is still less than the desired spring rate, which does reduce the range of stiffness that can be achieved in this variable stiffness actuator.

4 Testing and Results

Two testing methods were used in evaluating the performance and repeatability of the VSA mechanism design. First, one half of the complete compliant actuator mechanism was tested to compare the performance of the mechanism with the desired quadratic force-deflection behavior that the mechanism was optimized to produce. Then, the full antagonistic VSA mechanism was tested to evaluate the mechanism's performance in producing and controlling the linear stiffness of the attached robot joint. These tests also evaluated the repeatability of the design in producing the same results in multiple test cases.

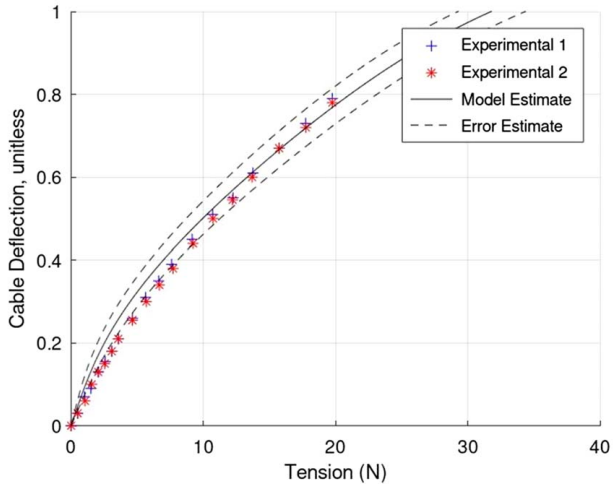

Fig. 12 Testing results for single-sided mechanism

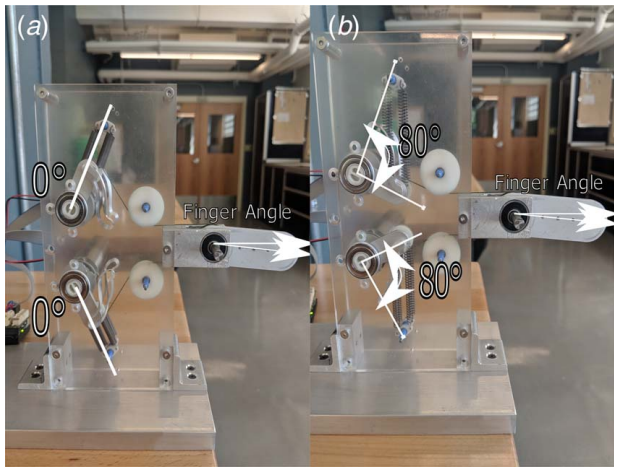

Fig. 13 Stiffness configuration examples

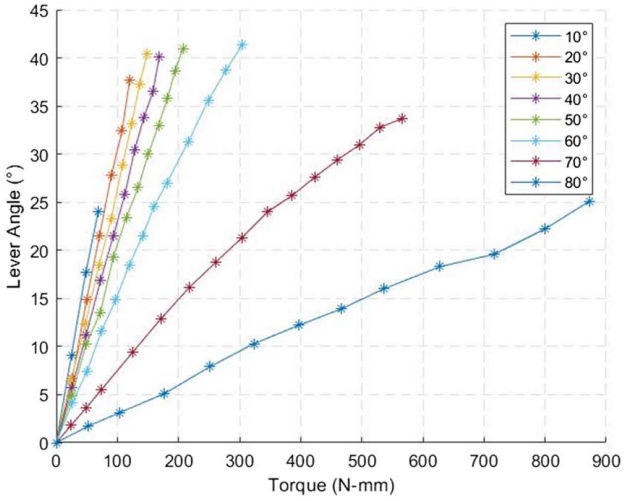

Fig. 14 Testing results for antagonistic mechanism

The lower half of the prototype mechanism shown in Fig. 10 was detached from the finger joint, and weights were attached to the cable to apply known static loads. Masses were added in 50 g increments to the end of the cable. For each mass added, the displacement of the cable was measured using a linear scale, resulting in a 0.5 mm resolution. Figure 12 shows the mechanism's cable deflection versus force curve of the mechanism compared to the expected curve calculated by the quasi-static model of the system. Additionally, reasonable error estimates of the model error are shown when incorporating a ±1 mm possible measurement error in the pretension value of the linear springs and a ±5% possible error in the measured linear spring rate. These are the two most likely sources of error between the simulated system values and the actual system performance.

The relative angle of the lever mechanism, θ_i, was measured using a potentiometer affixed to the base frame of the testing apparatus. The data matched the modeled behavior and show that the quasi-static model of the system matches the real-world testing apparatus reasonably well.

The second set of experiments involved both the top and bottom halves of the VSA mechanism being antagonistically attached to the robot finger joint. The motors controlling the VSA were set to various positions to create specific finger stiffness and finger joint position combinations. The finger joint was set at angles of −20 deg, 0 deg, and +20 deg relative to horizontal. Additionally, the stiffness of the finger was set by co-activating the motors to shorten the cables attached to the finger on either side incrementally. Each incremental step in stiffness increased the lever angle, θ_i, by 10 deg. Two examples of stiffness positions can be seen in Fig. 13, with Fig. 13(*a*) being the zero-stiffness position and Fig. 13(*b*) being a very stiff position.

A suite of tests in which a known torque was applied to the joint, and the deflection of the joint from its equilibrium position was recorded. The suite included three joint equilibrium positions and eight values of selected stiffness.

Results from the antagonistic testing of the VSA design are shown in Fig. 14 for the case in which the finger initial (equilibrium) angle was in a horizontal position (0 deg). The results show acceptable linearity in each test. When converted to translational quantities, the effective stiffness of the mechanism (at the cable end) ranged from approximately 2.7 N/mm to a maximum measured stiffness of 38 N/mm. The mechanism was able to achieve stiffnesses higher than 38 N/mm; however, because the joint angle deflection was so small, the data were not clear enough to confidently draw conclusions regarding stiffness linearity or repeatability and therefore is not presented here.

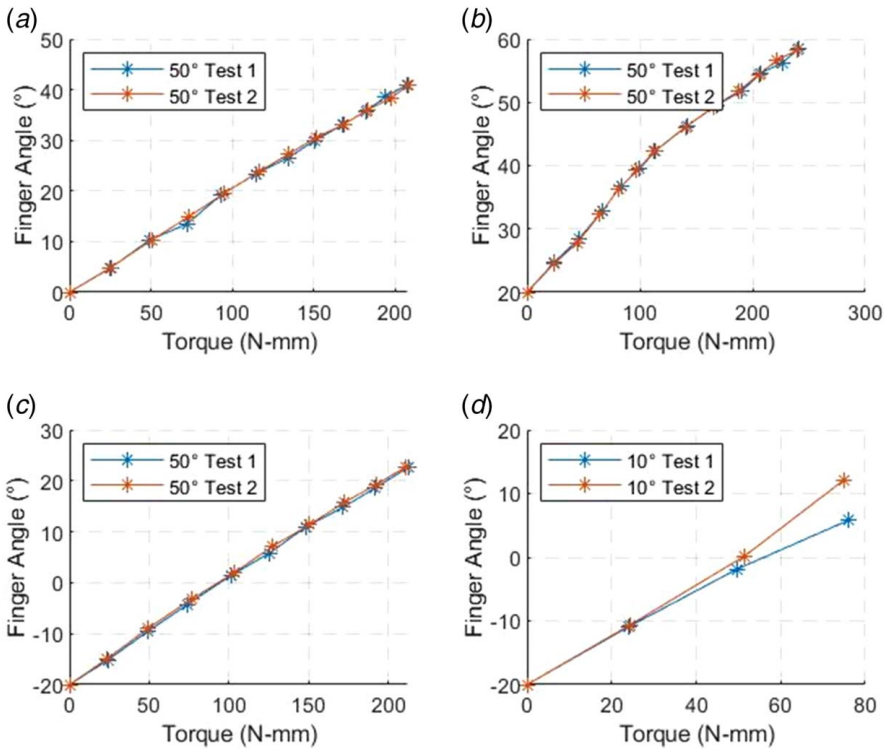

Fig. 15 Lever mechanism results: (*a*) 50 deg stiffness position, 0 deg finger angle position, (*b*) 50 deg stiffness position, +20 deg finger angle position, (*c*) 50 deg stiffness position, −20 deg finger angle position, and (*d*) 10 deg stiffness position, and 0 deg finger angle position

Consistency and repeatability of the mechanism performance were also tested through duplicate tests with the same load and the same selected stiffness. Figure 15 shows representative samples of the repeated tests for different selected stiffnesses. Figures 15(*a*)–15(*c*) show repeated tests of the same stiffness (50 deg input, moderate stiffness) with initial finger angles of 0 deg, 20 deg, and −20 deg, respectively. Figure 15(*d*) shows a repeated test of a lower stiffness (10 deg input). Figures 15(*a*)–15(*c*) show good consistency between tests; whereas, Fig. 15(*d*) shows some discrepancy in repeated testing, especially in the highest load case (the largest discrepancy found in all test cases run). In general, discrepancies were larger in the low stiffness configurations of the mechanism. These discrepancies are likely due to the larger relative impact of friction in the measurement system (the potentiometers) in the lower mechanism stiffness cases.

5 Conclusion

The objective of this project was to design a variable stiffness actuator that would have a large range of controllable linear stiffness while also controlling the position of a robot finger joint. The utilization of parametric optimizations to a design similar to the DLR's FAS design allowed for an understanding of the role each mechanism geometric parameter plays in creating the nonlinear behavior. The optimized design was constructed and tested. The prototype exhibited the desired controllable linear stiffness at the joint. This linear stiffness allows for a simplification of the modeling and control of the VSA when implemented into a manipulation system.

The next steps for this work include incorporating the design into a multi-joint finger and eventually a multi-finger hand with modifications to the structure of the design in order to house the required antagonistic mechanism and motors into an effective configuration. Additionally, a cable routing design will need to be worked in order to ensure that joints on the same finger do not interact with each other in a way that affects the linear stiffness that these mechanisms are designed to create.

Acknowledgment

This work was supported in part by the National Science Foundation under Grant IIS-427329.

Conflict of Interest

There are no conflicts of interest.

Data Availability Statement

Data provided by a third party are listed in Acknowledgment.

References

[1] Bekey, G., Ambrose, R., Kumar, V., Sanderson, A., Wilcox, B., and Zheng, Y., 2006, "International Assessment of Research and Development in Robotics," World Technology Evaluation Center, Inc.

[2] Watson, P. C., 1978, "Remote Center Compliance System," US4098001A.

[3] Ham, R. V., Sugar, T. G., Vanderbought, B., Hollander, K. W., and Lefeber, D., 2008, "Compliant Actuator Designs: Review of Actuators with Passive Adjustable Compliance/Controllable Stiffness for Robotic Applications," IEEE Rob. Autom Mag., **15**(3).

[4] Wolf, S., Eiberger, O., and Hirzinger, G., 2011, "The DLR FSJ: Energy Based Design of a Variable Stiffness Joint," IEEE International Conference on Robotics and Automation, Shanghai, China, May 9–13.

[5] Grebenstein, M., Albu-Schaffer, A., Bahls, T., Chalon, M., Eiberger, O., Friedl, W., Gruber, R., Haddadin, S., Hagn, U., Haslinger, R., and Höppner, H., 2011, "The DLR Hand Arm System," IEEE International Conference on Robotics and Automation, Shanghai, China, May 9–13.

[6] Friedl, W., Chalon, M., Reinecke, J., and Grebenstein, M., 2011, "FAS A Flexible Antagonistic Spring Element for a High Performance Over Actuated Hand," IEEE/RSJ International Conference on Intelligent Robots and Systems, San Francisco, CA, Sept. 25–30.

[7] Laurin-Kovitz, K. F., Colgate, J. E., and Carnes, S. D. R., 1991, "Design of Components for Programmable Passive Impedance," International Conference on Robotics and Automation, Sacramento, CA, Apr. 9–11.